Screen-Printed Graphene Film Circuit Model for Microwave Applications

Screen-Printed Graphene Film Circuit Model for Microwave Applications

Fabio Peinetti
Dept. of Electronic and Telecom.
Politecnico di Torino
Torino, Italy
fabio.peinetti@polito.it

Simone Quaranta
Istituto materiali nanostrutturati
CNRISMN
Roma, Italy
simone.quaranta@cnr.it

Patrizia Savi
Dept. of Electronic and Telecom.
Politecnico di Torino
Torino, Italy
patrizia.savi@polito.it

***Abstract*—Graphene, a 2D structure with carbon atoms arranged in a hexagonal (honeycomb) lattice, exhibits intriguing mechanical, thermal and electrical properties. Graphene nanoplatelets can be deposited on different substrates through the preparation of inks with a proper combination of solvents and binders. Films loaded with graphene are attractive for many applications as biosensors and chemical sensors as well as flexible electronics applications.**

In this paper, graphene films loaded with graphene nanoplateletes of weight fraction 25% are deposited by screen printing technique on a microstrip circuit and they are characterized in the microwave frequency range. By fitting the measured scattering parameters of graphene-loaded microstrip lines with Cadence AWR software simulations, an equivalent lumped circuit model of the film is obtained.

***Index Terms*—Graphene, Gap Model, Circuital Model, Nanoplatelets, Radio Frequency (RF), Screen Printing, Thick film**

I. Introduction

Graphene-based nano-materials have gained a large amount of interest for many applications in the optical range [1], and for RF and millimeter applications [2], [3], humidity sensors [4], [5], glucose sensors [6]–[9], components [10]–[12] and flexible electronics [13]. However, there has been little research done on the characterization of graphene films at microwave frequencies [14], [15], making it difficult to realize adequate electromagnetic models. Films loaded with graphene nanoplatelets can be deposited on different substrates through the preparation of inks with a proper combination of solvent and binders [16].

In many applications a graphene film can be easily described by using its sheet resistance. As demonstrated by several works (see e.g. [17]),the real part of the impedance of this type of materials is influenced by variations in the actual composition of the compound: an increase in graphene weight fraction corresponds to a reduction of the resistance and vice-versa. On the other hand, the simple sheet resistance model seems to be an insufficient approximation when dealing with more complex circuits.

In this paper a lumped circuital model is developed, to overcome the limitations of the definition of a sheet impedance in microwave analysis. The proposed circuit was simulated in order to fit measured S-parameters of a graphene weight-fraction 25% film deposition, in the range 1 GHz to 4 GHz. The simulations were performed on AWR software, from Cadence. The difference between simulated and measured S-parameters is lower than 1 dB in the whole frequency range. This equivalent lumped circuit model can replace and improve the sheet resistance description in full-wave electromagnetic simulation of graphene loaded microwave structures.

II. Microstrip circuit

In order to model screen-printed graphene films, a simple microstrip circuit was introduced. A copper microstrip line, 35 mm long, was etched on FR4 substrate of thickness (H) 1.57 mm, $\epsilon_r = 3.9,\ tan(\gamma) = 0.03,\ \rho_{FR4} = 17.24$ m$\Omega \cdot \mu$m. A gap of 3 mm was left in the middle in order to host the graphene film (see Fig. 1), whose size was actually 2.6 mm (S in the following discussion), since 0.2 mm are over-imposed to the lines, on each side, in order to guarantee an electric connection. The width (W) of the microstrip lines on both the sides is 3 mm in order to obtain a characteristic impedance of 50 Ohm.

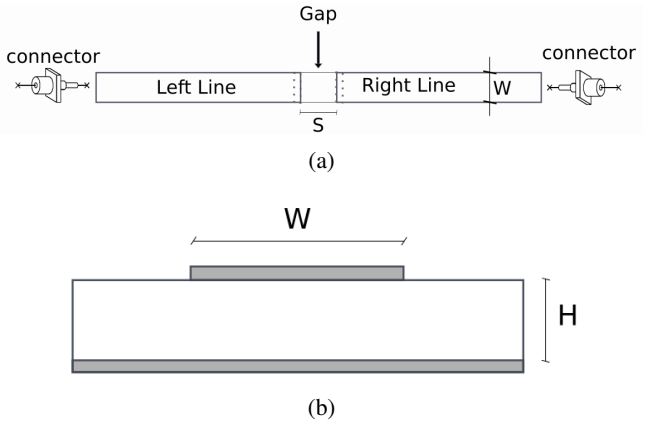

Fig. 1: Top (a) and lateral (b) view of the used microstrip circuit.

III. Graphene film deposition

Screen-printing is used to deposit graphene (Nanoinnova) as a thick film on a FR4 substrate across the gap between the two lines (see Fig.1). Ethyl cellulose (Sigma Aldrich,

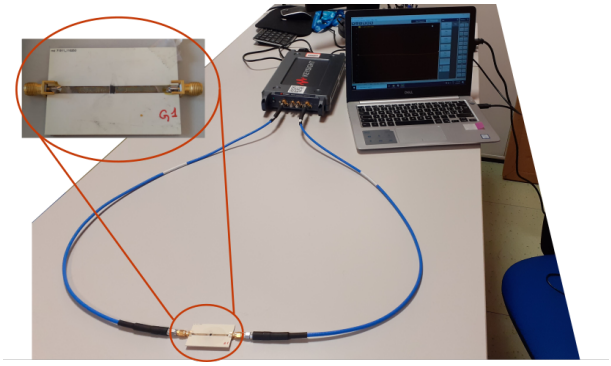

Fig. 2: Measurement setup: Vector Network Analyzer by Keysight (P9372A) and DUT connection.

viscosity 10 cP, 5% toluene/ethanol, 48% ethoxyl) is used as a binder dispersion steric stabilizer (see Fig: 4). It is dispersed in 80 mL of ethanol by stirring (2 hours) and sonication (15 hours by using a Ti horn) with a solvent, terpineol (Sigma Aldrich), and 25 wt.% graphene flakes. Ethanol is evaporated under reduced pressure in order to produce a printable paste. The ink's final formulation is comprised of graphene (25 wt%), ethyl cellulose (9.5wt%) and terpineol (65.5%). A 3 x 3 mm^2 film is printed on FR4 substrate through a polyester mesh screen. Each printed layer is dried at 125°C for 5 minutes after the deposition. Final curing is performed in a muffle at 120°C for 150 minutes in air [17]. Each layer is approximately 10 micron thick. Multiple layers structures can be obtained by repeating the previous procedure. The chemistry of ink formulation for screen printing accounts for a homogeneous dispersion of graphene flakes into the binder matrix. Homogeneous dispersion also guarantees repeatability of the films. A Tencor Alpha-Step-200 profilometer equipped with a standard stylus of 12.5 μm radius was used to measure the film thickness.

In Fig. 3 Scanning Electron Microscope (SEM) of screen-printed graphene film with graphene weight fraction 25% are shown with magnification of 10 μm, 2 μm and 1 μm. They indicate that the graphene flakes are uniformly dispersed throughout the film.

IV. Model Description

In this section, it is proposed a model for screen-printed graphene film (weight fraction 25%). Graphene can not be separated from the binder, which serves as interconnection and adhesion element, ensuring the printability of the ink. Moreover, the thermal treatment does not remove the ethyl-cellulose binder. For this reason, a preliminary analysis on a film made with the binder alone was performed. The red dotted box represents the "core" of the model. It models the gap and the binder deposition (fig 5). When modeling the graphene deposition (fig: 6), the elements in the green box should be added and the values of the elements in the red box are modified to keep into account the addition of graphene (the topology is left unaltered. Compare fig 5 and fig: 6).

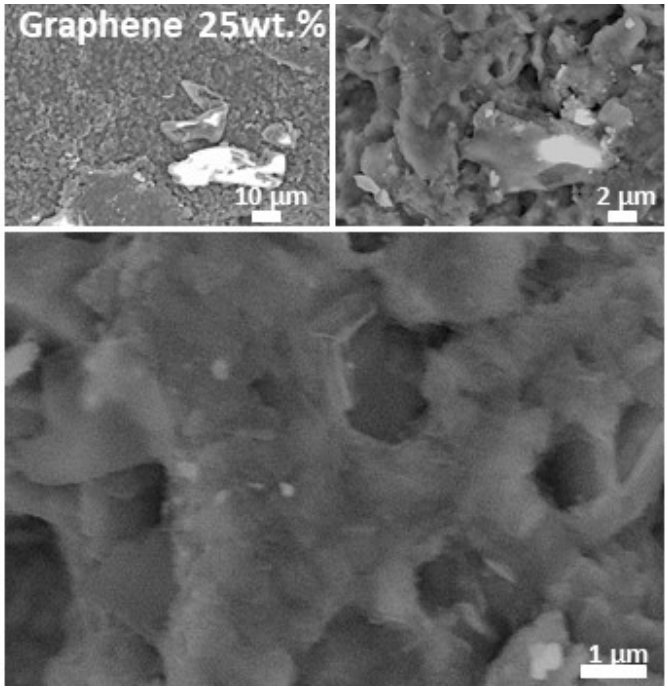

Fig. 3: Scanning Electron Microscope (SEM) of film with graphene (weight fraction 25%).

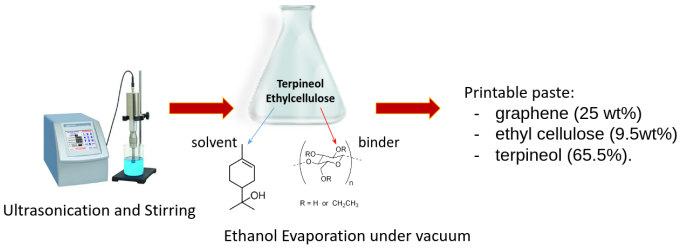

Fig. 4: Graphene (weight fraction 25%) ink preparation flow.

The pi network formed by (C_g, C_{gl}, C_{gr}) represents the gap. The inductance L_g and the resistances keep into account the deposition and its losses.

The values of the elements of the circuit change since the actual chemical composition of the deposited film is changed, as well as the corresponding physical properties.

The final model taking into account both the binder and the graphene film is shown in Fig. 6. In particular a reduction in the sheet resistance can be expected, due to the increase in percolative paths. In Fig. 6 (green-squared box), there is a parallel capacitor C_{pp}; the capacitance C_{pp} accounts for the creation of nanoscale capacitors, whose conductive element is the graphene platelet and binder acts as dielectric material [16], [17]. Furthermore a RC series element is added at the output node.

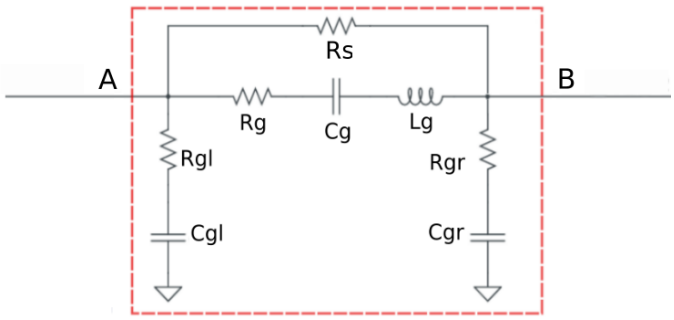

Fig. 5: Circuit model for the binder deposition.

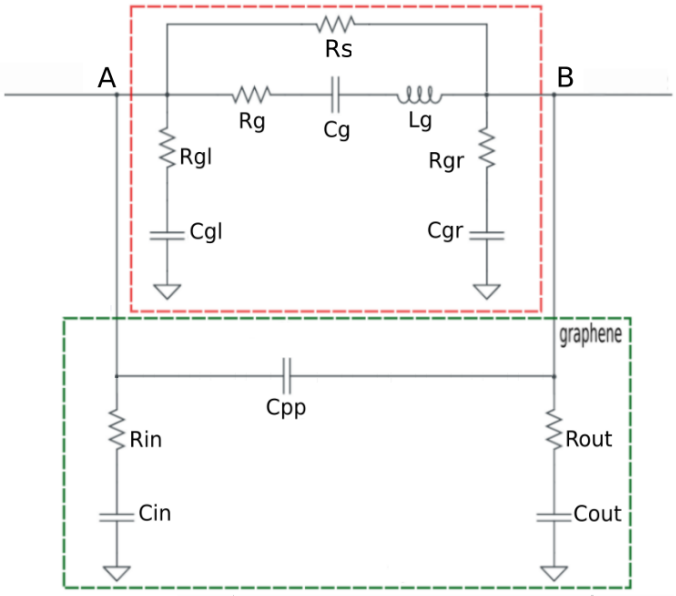

Fig. 6: Circuit model for the graphene plus binder deposition (graphene weight fraction 25%).

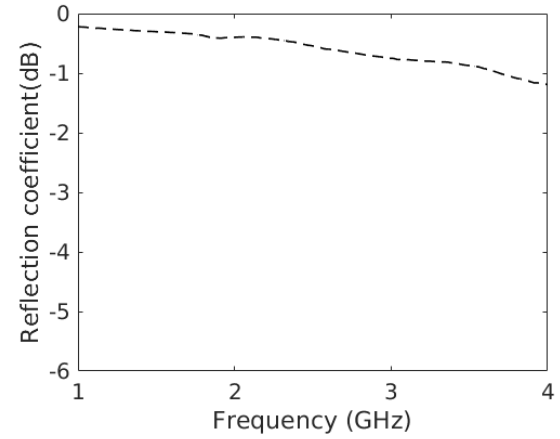

(a)

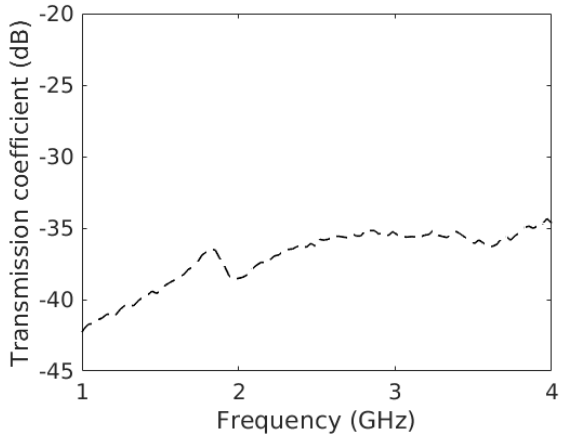

(b)

Fig. 7: Binder-filled gap: measured reflection (a) and transmission (b) coefficients.

V. Results and Discussion

The scattering parameters of the microstrip lines with the film (binder alone and binder with graphene) are measured from 1 GHz to 4 GHz with a USB 2-port Vector Network Analyzer by Keysight (P9372A characterized by a frequency band from 300 kHz to 9 GHz) (Fig: 2). In order to compensate for systematic errors, the VNA is calibrated through an electronic calibration kit (N7551A), which implements the standard calibration termination: open and short circuits and a 50 Ω load. Thanks to the calibration procedure, the reference planes are moved in correspondence of DUT's connectors and compensated for the coaxial cables delay, transitions filtering effects, etc... The samples were measured several times and in the following, the reported plots, represent the average curves of all the measurements.

Fig: 7 shows reflection and transmission coefficients measured for a binder-filled gap. As expected, the presence of ethyl-cellulose does not cause a significant variation with respect to the case of an unfilled gap. The reflection coefficient is close to 0 dB due to the matched 50 Ω line. The decrease in frequency is due to losses in the dielectric. The transmission coefficient below −30 dB is due to signal attenuation between the two ports as expected.

In Fig. 8a and Fig. 8b the magnitude and phase of the measured reflection coefficient for a graphene (wt. 25%) ink are reported, while in Fig. 9a and Fig. 9b the transmission coefficients are shown (dashed lines). The S-parameters (S_{12} and S_{22}) are not shown since they are similar to (S_{21} and S_{11}, respectively). As it was expected, the binder film has no impact on the S-parameters response. This is due to the fact that the relative dielectric constant and the loss tangent of the cellulose derivative binders are of the same order of FR4 [16]. Measurements (dashed line) and model-derived fitted data (solid line) are compared in Fig. 8a-Fig. 9b for the graphene-filled gap. Good agreement is observed between the measurements and the circuit model over range 1 GHz to 4 GHz. A maximum error of 0.5 dB is obtained in the case of the transmission coefficients. A difference between

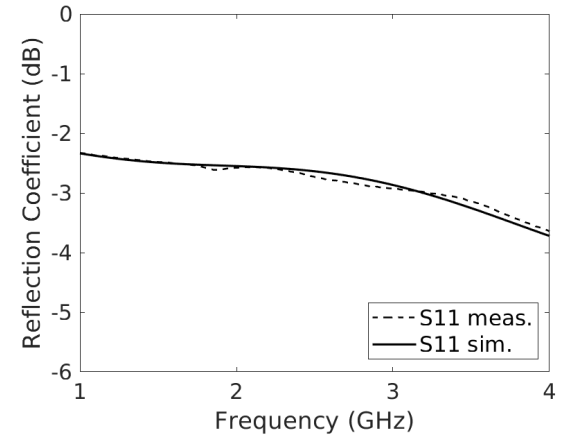

(a)

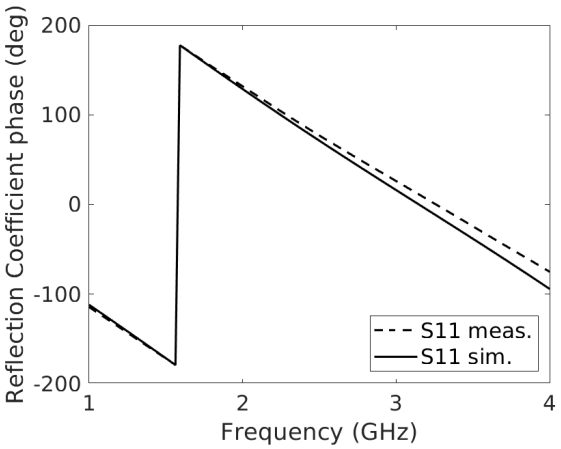

(b)

Fig. 8: Graphene-filled gap: measured reflection coefficient (dashed line) and simulated (solid line). (a) magnitude (b) phase.

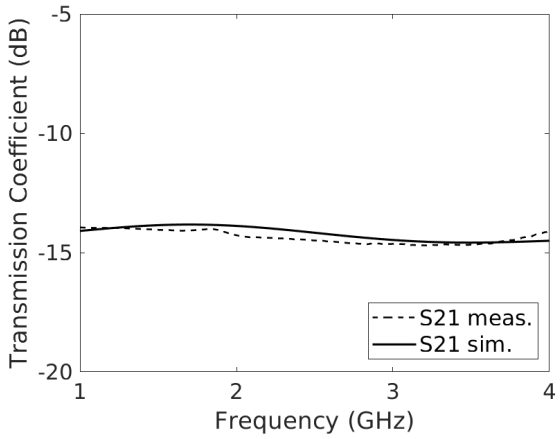

(a)

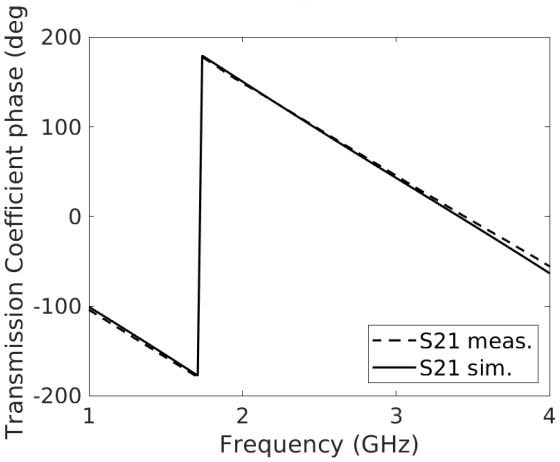

(b)

Fig. 9: Graphene-filled gap: measured transmission coefficient (dashed line) and simulated (solid line). (a) magnitude (b) phase.

measured and simulated parameters lower than 0.25 dB, in the whole frequency range is obtained in the case of the reflection coefficients S_{11} and S_{22}.

Tables I and II report the values of the parameters used in the simulations. The "Core" covers the elements inside the red squared area in Fig:6, while the "Other elements" are those included in the green box. As it was expected, the overall resistance, between node A and B, falls from 43 kΩ to 442.4 Ω, due to the increase in percolative paths; the same reasoning holds for the series resistance R_g and the other resistive elements. Converting R_s into a more generalized form with (1), the resulting sheet resistance is 442.4 $\Omega/\square$ (with a unitary aspect ratio):

$$R_{sheet} = R_s \cdot \frac{W}{L} \tag{1}$$

From [16] a two layer ethyl-cellulose graphene wt. 25% compound, namely the same used here, is characterized by a DC 440 $\Omega/\square$ resistance. The result is also confirmed by [17], performing an HFSS (High Frequency Structure Simulator, Canonsburg, PA, USA) full wave-analysis with a surface resistance $\Re\{Z_{sheet}\} = 450$ Ω for a deposition of 3 mm $\times$ 3 mm.

TABLE I: Electrical model parameters - "Core"

	R_s (kΩ)	R_g (kΩ)	C_g (pF)	L_g (pH)
Graphene wt. 25%	0.422	1	0.032	15.8

	R_{gl} (Ω)	C_{gl} (pF)	R_{gr} (Ω)	C_{gr} (pF)
Graphene wt. 25%	28	0.085	28	0.085

TABLE II: Electrical model parameters - "Other elements"

	R_{in} (Ω)	C_{in} (pF)	R_{out} (Ω)	C_{out} (pF)	C_{pp} (pF)
Graphene wt. 25%	36	0.2	36	0.2	0.029

VI. Conclusion

Microstrip lines with a gap on which is screen-printed a film with graphene of weight fraction of 25% is analyzed. By fitting the measured S-parameters with simulated data obtained with AWR, a circuit model is proposed in the 1 GHz to 4 GHz range. This model could also be applied to graphene compounds with a different weight-fraction.

When dealing with graphene films, the difference between simulated and measured S-parameters is lower than 0.5 dB in the whole frequency range.

The equivalent lumped circuit model presented in this paper proves suitable as an initial step towards the full-wave electromagnetic modeling and analysis of graphene loaded microwave structures intended for sensing and tuning applications. The model could improve simulation results, where the graphene compound is represented as a simple sheet resistance, such as gas or glucose sensors. A de-embedding procedure could be developed so to differentiate the contributions of graphene and binder.

The model could be improved so to correctly describe the behavior in correspondence of an applied voltage. This may lead to more complex applications, such as RF controllable and tunable devices [18].

References

[1] F. Bonaccorso, Z. Sun, T. Hasan, and A. Ferrari, "Graphene photonics and optoelectronics," *Nature photonics*, vol. 4, no. 9, pp. 611–622, 2010.

[2] E. W. Hill, A. Vijayaragahvan, and K. Novoselov, "Graphene sensors," *IEEE Sensors Journal*, vol. 11, no. 12, pp. 3161–3170, 2011.

[3] M. Bozzi, L. Pierantoni, and S. Bellucci, "Applications of graphene at microwave frequencies," *Radioengineering*, vol. 24, no. 3, pp. 661–669, 2015.

[4] X. Leng, W. Li, D. Luo, and F. Wang, "Differential structure with graphene oxide for both humidity and temperature sensing," *IEEE Sensors Journal*, vol. 17, no. 14, pp. 4357–4364, 2017.

[5] D. Lei, Q. Zhang, N. Liu, T. Su, L. Wang, Z. Ren, Z. Zhang, J. Su, and Y. Gao, "Self-powered graphene oxide humidity sensor based on potentiometric humidity transduction mechanism," *Advanced Functional Materials*, vol. 32, no. 10, p. 2107330, 2022.

[6] Z. Zhu, L. Garcia-Gancedo, A. J. Flewitt, H. Xie, F. Moussy, and W. I. Milne, "A critical review of glucose biosensors based on carbon nanomaterials: carbon nanotubes and graphene," *Sensors*, vol. 12, no. 5, pp. 5996–6022, 2012.

[7] R. Reghunath, K. Singh *et al.*, "Recent advances in graphene based electrochemical glucose sensor," *Nano-Structures & Nano-Objects*, vol. 26, p. 100750, 2021.

[8] M. Dragoman, D. Neculoiu, A.-C. Bunea, G. Deligeorgis, M. Aldrigo, D. Vasilache, A. Dinescu, G. Konstantinidis, D. Mencarelli, L. Pierantoni *et al.*, "A tunable microwave slot antenna based on graphene," *Applied Physics Letters*, vol. 106, no. 15, p. 153101, 2015.

[9] Y. Kim, J. B. Park, Y. J. Kwon, J.-Y. Hong, Y.-P. Jeon, and J. U. Lee, "Fabrication of highly conductive graphene/textile hybrid electrodes via hot pressing and their application as piezoresistive pressure sensors," *Journal of Materials Chemistry C*, vol. 10, no. 24, pp. 9364–9376, 2022.

[10] G. R. Hotopan, S. Ver Hoeye, C. Vazquez, R. Camblor, M. Fernández, F. Las Heras, P. Álvarez Rodríguez, and R. M. Menéndez López, "Millimiter wave microstrip mixer based on graphene," 2011.

[11] G. R. Hotopan, S. Ver-Hoeye, C. Vazquez-Antuna, A. Hadarig, R. Camblor-Diaz, M. Fernandez-Garcia, and F. L. H. Andres, "Millimeter wave subharmonic mixer implementation using graphene film coating," *Progress In Electromagnetics Research*, vol. 140, pp. 781–794, 2013.

[12] M. Yasir, P. Savi, S. Bistarelli, A. Cataldo, M. Bozzi, L. Perregrini, and S. Bellucci, "A planar antenna with voltage-controlled frequency tuning based on few-layer graphene," *IEEE Antennas and wireless propagation Letters*, vol. 16, pp. 2380–2383, 2017.

[13] N. Haider, D. Caratelli, and A. Yarovoy, "Recent developments in reconfigurable and multiband antenna technology," *International Journal of Antennas and Propagation*, vol. 2013, 2013.

[14] M. Liang, M. Tuo, S. Li, Q. Zhu, and H. Xin, "Graphene conductivity characterization at microwave and thz frequency," in *The 8th European Conference on Antennas and Propagation (EuCAP 2014)*. IEEE, 2014, pp. 489–491.

[15] J. Obrzut and A. C. Moraes, "Microwave characterization of graphene inks," 2021.

[16] O. Sanusi, P. Savi, S. Quaranta, A. Bayat, and L. Roy, "Equivalent circuit microwave modeling of graphene-loaded thick films using s-parameters," *Progress In Electromagnetics Research Letters*, vol. 76, pp. 33–38, 2018.

[17] S. Quaranta, M. Miscuglio, A. Bayat, and P. Savi, "Morphological and radio frequency characterization of graphene composite films," *C*, vol. 4, no. 2, p. 32, 2018.

[18] M. Yasir, S. Bistarelli, A. Cataldo, M. Bozzi, L. Perregrini, and S. Bellucci, "Enhanced tunable microstrip attenuator based on few layer graphene flakes," *IEEE Microwave and Wireless Components Letters*, vol. 27, no. 4, pp. 332–334, 2017.

[19] W. J. Hyun, E. B. Secor, M. C. Hersam, C. D. Frisbie, and L. F. Francis, "High-resolution patterning of graphene by screen printing with a silicon stencil for highly flexible printed electronics," *Advanced Materials*, vol. 27, no. 1, pp. 109–115, 2015.

[20] C. Joseph, F. Luzi, S. Azman, P. Forcellese, E. Pavoni, G. Fabi, D. Mencarelli, S. Gentili, L. Pierantoni, A. Morini *et al.*, "Nanoscale characterization of graphene oxide-based epoxy nanocomposite using inverted scanning microwave microscopy," *Sensors*, vol. 22, no. 24, p. 9608, 2022.